THE JOURNAL OF PHYSICAL CHEMISTRY C

Article

pubs.acs.org/JPCC

Supramolecularly Modified Graphene for Ultrafast Responsive and Highly Stable Humidity Sensor

Shiwei Wang,[∥,†] Zhuo Chen,[∥,†] Ahmad Umar,[‡] Yao Wang,[*,†] Tong Tian,[†] Ying Shang,[†] Yuzun Fan,[†] Qi Qi,[§] and Dongmei Xu[§]

[†]Key Laboratory of Bio-Inspired Smart Interfacial Science and Technology of Ministry of Education, School of Chemistry and Environment, Beihang University, Beijing 100191, PR China

[‡]Department of Chemistry, Faculty of Science and Arts and Promising Centre for Sensors and Electronic Devices (PCSED), Najran University, Najran 11001, Kingdom of Saudi Arabia

[§]Gas and Humidity Sensing Department, Beijing Elite Tech Co., Beijing 100850, PR China

Supporting Information

ABSTRACT: We report the fabrication and detailed characterization of an ultrafast responsive, excellently stable and reproducible humidity sensor based on a supramolecularly modified graphene composite. The fabricated humidity sensors exhibited a response and recovery time of less than 1 s, which is the lowest among the values found in the literature. In addition, various sensing performances of the fabricated humidity sensors were studied in detail, and the corresponding kinetic model and mechanism have also been deduced and described.

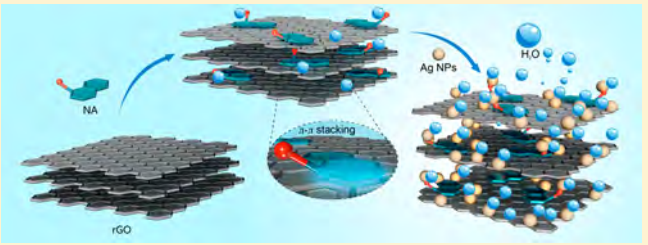

INTRODUCTION

Recently, humidity sensors (HSs) have attracted considerable attention because of their wide practical and potential industrial applications in the areas of production, process control, environmental monitoring, storage, and so on.[1,2] An ideal HS should be cost-effective and possess high sensitivity, quick response time, broad operational range, and excellent durability and reproducibility.[3] Recently, the performance of HSs, in terms of sensitivity and reproducibility, have been improved to a certain extent.[4−6] However, it is still a challenge to fabricate efficient HSs with ultrafast response and high stability toward relative humidity (RH).[7]

Graphene oxide (GO) is a novel carbon material which possesses excellent properties and is therefore used in a variety of applications, for example, analysis and detection, biomedicine, polymer modifications, electronics, and optoelectronics,[8,9] to name but a few. Because of the very particular and interesting properties of GO, such as a two-dimensional (2D) platform structure with numerous oxygen functional groups on the basal plane and its edges, such as hydroxyl, epoxy groups, and carboxylic acid groups, which are highly hydrophilic and reactive groups, GO-based materials are considered to be good candidates for fabricating efficient HSs.[10−21]

These intrinsic properties make GO-based materials a promising candidate for fabricating efficient humidity nanosensors.[17−21] A survey of the literature revealed that covalently bonding with functional molecules was usually chosen as a major approach to obtain functionalized GO materials for efficient sensor applications.[22] However, it is known that during chemical modifications, the original perfect atomic lattices of pristine GO can be affected by chemical bonds which seriously affect the intrinsic electrical properties of graphene.[23] Therefore, to avoid such drawbacks, supramolecular assembly based on the noncovalent interactions is an alternative way which does not show any chemical effect on the intact structure of GO because of the noncovalent interaction.[24,25] Importantly, to the best of our knowledge, such an approach of modifying GO using small-molecule supramolecular modification (SM) and its application in humidity sensors has never been reported in the literature.

This work reports the successful fabrication and characterization of an ultrafast responsive and highly stable humidity sensor based on supramolecularly modified graphene with naphthalene-1-sulfonic acid sodium salt (NA) and silver nanoparticles (Ag). Interestingly, the fabricated HS based on Ag-NA-rGO (where rGO indicates reduced graphene oxide) composite exhibited extremely excellent sensing characteristics, including ultrafast response and recovery time (≤1 s) for measuring RH between 11% and 95% in air at room temperature (25 °C) with the test frequency at 100 Hz, which have reached the record limit of the operating instrument. Furthermore, the fabricated HS exhibited quite high stability and reproducibility. The ultrafast response of the fabricated HS can be attributed to the introduction of a

Received: September 8, 2015
Revised: November 18, 2015
Published: November 25, 2015

DOI: 10.1021/acs.jpcc.5b08771
J. Phys. Chem. C 2015, 119, 28640−28647

Scheme 1. Typical Schematic for the Fabrication Process of Ag-NA-rGO Composites

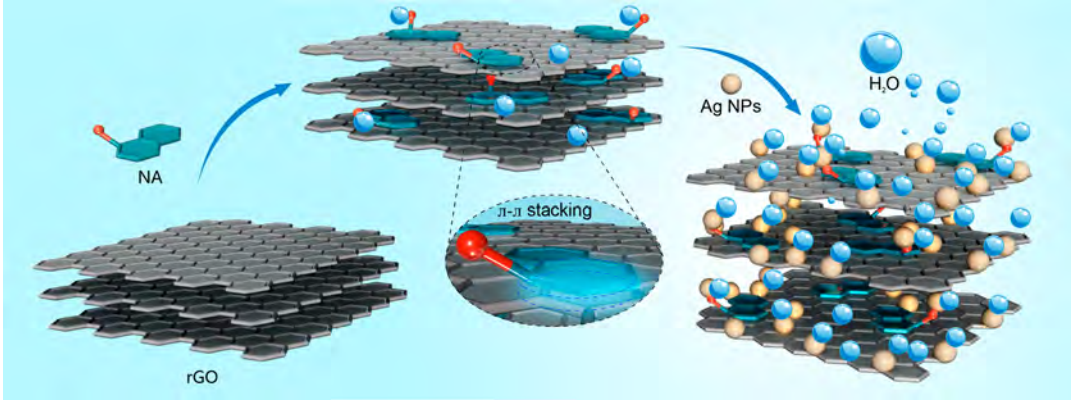

multiple-layer assembly system. Importantly, a corresponding mathematical mechanistic modeling of supramolecular assembly on rGO with small organic molecules and metallic nanoparticles has also been proposed and is presented in this paper.

EXPERIMENTAL SECTION

Preparation of Graphene Oxide. GO was purchased from XianFeng NANO Co., Ltd. in China. To get uniform GO dispersion of 1 mg/mL, 100 mg of GO flake was dispersed in 100 mL of deionized (DI) water by sonication for 30 min.

Preparation of Reduced Graphene Oxide. In the preparation of rGO, 4 mL of GO dispersion was diluted by adding 16 mL of DI water; 75 μL of ammonia (30%) was then added to regulate pH to 12.5, and 10 mL of hydrazine hydrate (1.12 μL/mL) was mixed as the reductant under sonication in a 50 mL round-bottom flask. Eventually, a stable rGO suspension was obtained by heating the mixture at 95 °C in an oil bath for 1 h.

Preparation of Naphthalene-1-sulfonic Acid Sodium (NA) Modified rGO (NA-rGO). In the preparation of NA-rGO, 4 mL of GO dispersion was diluted by adding 10 mL of DI water in a 50 mL round-bottom flask which formed a uniform brown dispersion. Subsequently, 92 mg of NA, 5 mL of NaOH solution (4 mg/mL), and 10 mL of hydrazine hydrate (1.12 μL/mL) were added in succession, and the mixture was further stirred at 80 °C for 1 h and then rinsed three times with DI water by vacuum filtration. After mild sonication, the NA-rGO membrane was redispersed in 20 mL of water.

Preparation of Ag-NA-rGO Composites. In the preparation of Ag-NA-rGO, 4 mL of GO dispersion was diluted by adding 10 mL of deionized water in a 50 mL round-bottom flask under stirring, which formed a uniform brown dispersion. Subsequently, 92 mg of NA and 16 mg of silver nitrate were added in succession under stirring. After dropwise addition of 5 mL of NaOH solution (4 mg/mL) and 10 mL of hydrazine hydrate (1.12 μL/mL), the mixture was further stirred for 1 h at 80 °C in an oil bath. Finally, the obtained mixture was rinsed three times with DI water by vacuum filtration. After mild sonication, the Ag-NA-rGO membrane was redispersed in 20 mL of water.

Fabrication of Humidity Sensors. Interdigitated electrodes (IEs) were used to fabricate the humidity sensors, which were made of a ceramic substrate (6 mm × 3 mm, 0.5 mm thick) with five pairs of Ag−Pd interdigitated electrodes (electrode width and distance: 0.15 mm). For the fabrication of humidity sensors, a drop and dry method was used as reported in the literature.[36] Specifically, 0.1 mL of rGO, NA-rGO, or Ag-NA-rGO suspensions (0.2 mg/mL) was dropped on the surface of the IE and dried in air at 60 °C for 5 h to form a thin membrane on the electrode surface. Finally, the different IEs were prepared for sensing measurements.

Characterizations. The surface properties of the prepared materials were examined by atomic force microscopy (AFM). The AFM analysis were done using a Dimension Icon instrument (United States). Raman-scattering spectra were recorded using a HORIBA Jobin Yvon Raman microscope (Lab RAM HR800) with a 514 nm laser at a power density of 4.7 mW. X-ray diffraction (XRD) measurements were performed to estimate the interlayer distance. X-ray photoelectron spectra (XPS) were measured using an ESCALAB250 photoelectron spectrometer (Thermo Fisher Scientific, United States). The morphological characterizations of the prepared composites were investigated by scanning electron microscopy (SEM; Quanta 250 FEG, FEI) and transmission electron microscopy (TEM; Sirion-200, Japan).

The humidity sensing properties were investigated with a ZL5 intelligent LCR test meter. The adopted humidity sensing experimental setup and methods were the same as those reported in the literature.[37,38] The characteristic curves of humidity response were measured on a CHS-1 Humidity Sensing Analysis System (Beijing Elitetech, China). The voltage applied in our studies was AC 1 V, and the frequency varied from 20 Hz to 100 kHz. The sensor was placed in several chambers with different RH levels at an operating temperature of 25 °C. The used humidity chambers were made from glass (17 cm in height and 10 cm in diameter). The six different saturated salt solutions were LiCl, $MgCl_2$, $Mg(NO_3)_2$, NaCl, KCl, and KNO_3, and their corresponding RH values were 11, 33, 54, 75, 85, and 95% RH, respectively. An automatic drier was used to maintain the laboratory atmosphere at 25% RH. Usually, 10 h were used to ensure the equilibrium state in the chamber for these investigations.

RESULTS AND DISCUSSION

Fabrication of the Graphene-Based Sensors. For the modification of GO, a functional organic molecule NA with a large planar aromatic conjugated structure and sulfophenyl ending groups (ph-SO_3^-) was selected as a typical electron-withdrawing group to form NA-rGO composite. Here, naphthalene rings in NA molecules are offering the intrinsic driving force of $\pi-\pi$ interactions with GO surfaces. The

DOI: 10.1021/acs.jpcc.5b08771
J. Phys. Chem. C 2015, 119, 28640−28647

negatively charged sulfophenyl groups in NA serve as the functional spots of hydrophilicity (Scheme 1). It was observed that the water solubility of both of the composites, i.e., NA-rGO and Ag-NA-rGO, were greatly improved because of the introduction of hydrophilic sulfophenyl groups and Ag nanoparticles, which simultaneously well resolved the puzzle of poor dispersibility of graphene.

Another highlight in the multilevel structure is the introduction of silver nanoparticles to form the Ag-NA-rGO, which could further isolate the graphene layers to enhance the specific surface area and improve the adsorption capacity in the system.[26−28,31,32] Precisely, the supramolecular driving force for importing silver ions (Ag^+) was electrostatic interaction, by which positively charged Ag^+ were assembled with the sulfophenyl (Ph-SO_3^-) on NA molecule and with carboxylic groups ($-COO^-$) on the surface of GO as well. Finally, the multilayers of the reduced graphene oxide with interbedded NA molecules and silver nanoparticles were obtained. Thus, because of the multidimensional structure, the fabricated Ag-NA-rGO-based HSs demonstrate excellent sensing performances.

Characterizations of Graphene-Based Sensors. To understand the detailed morphology, the prepared Ag-NA-rGO composites were characterized by transmission electron microscopy (TEM). Figure 1A,B exhibits the typical TEM images of prepared Ag-NA-rGO composite which confirmed the uniform dispersion of silver nanoparticles over rGO. The typical diameters of the silver nanoparticles were in the range of 17 ± 3 nm. Importantly, lamellar Ag-NA-rGO composite have been formed with the introduction of interbedded Ag nanoparticles, as can be seen from SEM images (Figure 1C). To investigate the morphologies, the prepared Ag-NA-rGO composites were further examined by atomic force microscopy (AFM), and the results are shown in Figure S1. From the observed AFM image, it is clear that the silver nanoparticles are dispersed in nanoscale range on the rGO sheets and the typical thickness of one single graphene layer was ∼0.8−1.0 nm. Interestingly, the AFM results are consistent with the TEM observations. The structure was highly beneficial for enlarging the contact areas of H_2O molecules, as discussed in the text.

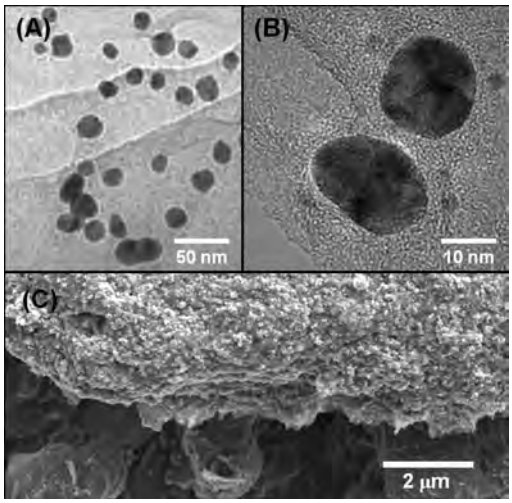

Figure 1. (A) Low- and (B) high-magnification TEM images of Ag nanoparticles over rGO; (C) SEM image for the corner portion of Ag-NA-rGO composite film.

Figure 2A exhibits the typical Raman-scattering spectrum for the Ag-NA-rGO composite, which shows different peaks compared to the Raman-scattering spectra of GO, rGO, and NA-rGO. The phonon peaks appearing at 1329 and 1597 cm^{-1} of Ag-NA-rGO composite were increased sharply, which are defined as the D-band and G-band. Additionally, the intensity ratios between D-band and G-band (ID/IG) of rGO, NA-rGO and Ag-NA-rGO were found to be 1.35, 1.34 and 1.35, respectively. Theoretically, with the higher ID/IG values, the graphene possess better structures and fewer defects. Interestingly, it was observed that the ID/IG values for the rGO, NA-rGO, and Ag-NA-rGO were higher than that of the GO (1.15); thus, it is clear that the prepared graphene-based materials possess better structures with significantly less structural defects.[41] Furthermore, it is also clearly confirmed that the functional groups in GO have been successfully and completely reduced. The successful reduction of GO also contributes to the promotion of conductivity.

Furthermore, the X-ray diffraction (XRD) measurements were done to estimate the interlayer distance of the three prepared composites. As shown in Figure 2B, the diffraction reflection for the (002) peak was moved from 2θ = 22.78° for NA-rGO to 2θ = 16.12° for Ag-NA-rGO. Thus, the interlayer distance between the layers of NA-rGO and Ag-NA-rGO were calculated and found to be ∼0.39 and 0.55 nm, respectively. The observed interlayer distance values are consistent with the reported literature.[39−41] In addition, the diffraction reflections appearing at 2θ = 38.34°,44.52°, 64.68°, and 77.58° correspond to Ag(111), Ag(200), Ag(220), and Ag(311), respectively, for the face-centered cubic (fcc) crystal form of Ag nanoparticles. The insertion of Ag nanoparticles slightly increase the interlayer distance from 0.39 to 0.55 nm, which is also the reason for the shift in 2θ from 22.78° to 16.12°.

To examine the surface and structural properties, all the prepared materials, i.e., rGO, NA-rGO, and Ag-NA-rGO were further characterized by X-ray photoelectron spectroscopy (XPS), and the observed results are shown in Figure 3. As evident from the observed XPS spectra, the sulfur (S_{2p}) peaks of NA-rGO and Ag-NA-rGO were obviously increased compared with that of rGO (Figure 3A), and the silver (Ag_{3d}) peaks in Ag-NA-rGO composite were obviously enhanced compared with the ones in rGO and NA-rGO (Figure 3B). Thus, the observed XPS results revealed that the NA molecules and Ag nanoparticles have been successfully assembled with rGO in Ag-NA-rGO composites through the supramolecular modifications.

Humidity Sensing Properties of the Graphene-Based Sensors. Figure 4 exhibits the impedance measurement curves for the Ag-NA-rGO composite-based HS under different RHs measured at different frequencies at room temperature (25 °C). The observed impedance results revealed the high humidity sensitivity and fast response in the entire RH range in the low-frequency region of 10 and 100 000 Hz. Taking into account that the commonly used frequency of HS devices is 100 Hz, the operational frequency for the experiments was chosen to be 100 Hz.

The response and recovery behavior is an important characteristic for evaluating the performance of HSs.[29,30] Figure 5 shows the hysteresis curve of Ag-NA-rGO-based sensor and response/recovery characteristic curves of the three kinds of graphene-based HSs for five cycles for RH from 11% to 95%. Interestingly, when the humidity was varied gradually from 11% to 95%, the fabricated Ag-NA-rGO-based HSs exhibited an

DOI: 10.1021/acs.jpcc.5b08771
J. Phys. Chem. C 2015, 119, 28640−28647

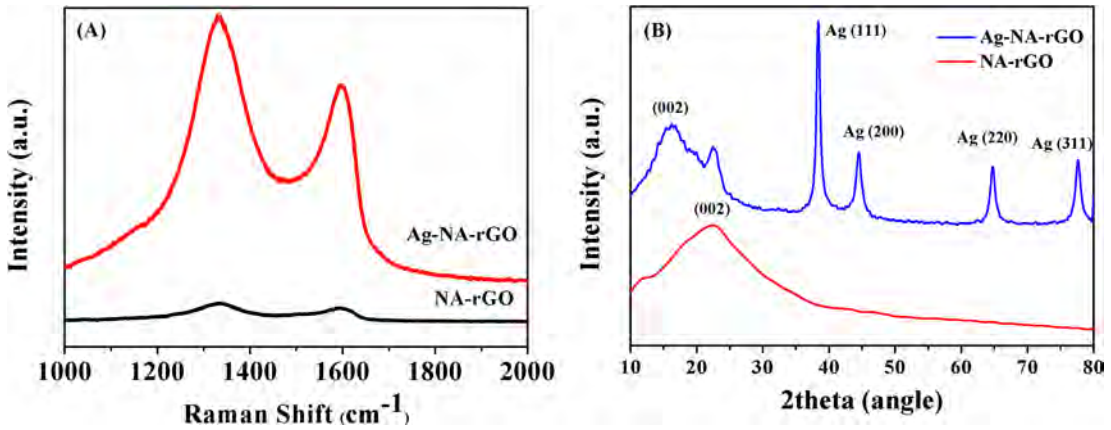

Figure 2. (A) Raman-scattering spectra of NA-rGO and Ag-NA-rGO composites; (B) XRD pattern of NA-rGO and Ag-NA-rGO composites.

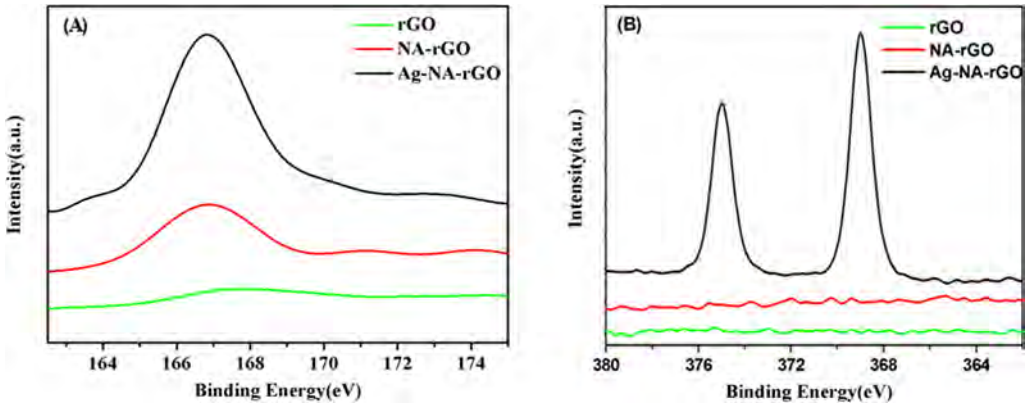

Figure 3. XPS results for GO, rGO, NA-rGO, and Ag-NA-rGO; (A) S_{2p} and (B) Ag_{3d} spectra.

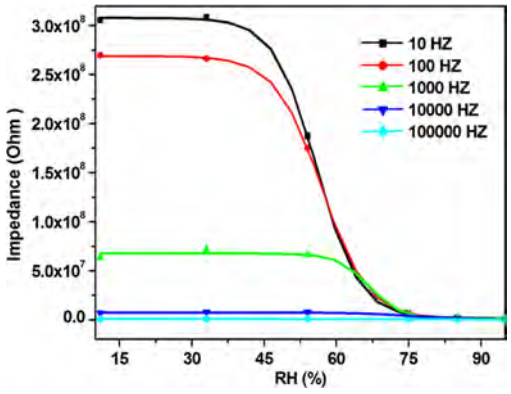

Figure 4. Impedance measurements curves for the Ag-NA-rGO composite-based HS under different RHs measured at different frequencies.

ultrafast response, less than 1 s, which was the record limit of the operating instrument. Interestingly, the sensitivity of the as-prepared HS reached a significant value 600 times under the test conditions at 100 Hz while the NA-rGO-based HS exhibited only 100 times, even though it also possessed a less than 1 s response time. It is worth mentioning that rGO-based HSs exhibited only 1.3 times with a longer response time, i.e., more than 50 s. The observed results revealed that the introduction of NA enhances the sensitivity and greatly shortens the response time, which could be further promoted with the assembly of Ag nanoparticles. Moreover, it is obvious that the Ag-NA-rGO-based HS exhibited an excellent hysteresis effect of 9%, as shown in Figure 5A. Consequently, the results confirmed the superior humidity sensing properties of the multilevel supramolecular structure of Ag-NA-rGO.

Stability is one of the important characteristics for an efficient HS used for practical applications. Thus, to check the stability, the fabricated Ag-NA-rGO composite-based HS was exposed in air for 110 days and the sensing performances such as response time and sensitivity at various RHs were examined. Interestingly, it was found that there was little change, within the error range, in the response time and sensitivity, which clearly revealed that the fabricated HSs based on Ag-NA-rGO composite possess very high stability at room temperature (Figure 6). Furthermore, the sensing performances of the fabricated HSs presented in this study were compared with that of the earlier reported HSs (Table S1). The detailed comparative studies revealed that the fabricated supramolecularly modified graphene-based composite (Ag-NA-rGO) exhibited outstanding humidity sensing characteristics such as ultrafast response and recovery time (≤1 s) and excellent reproducibility and stability (110 days) at room temperature (25 °C).

Thus, the characteristics and performance of the fabricated HSs demonstrated in this paper have surpassed the performance of all previously reported humidity sensors,[4−7,34,35] as revealed in Table 1; a more detailed comparative analysis is provided in the Supporting Information.

Mechanism of the Humidity Sensing. The properties of HS are mainly based on the changes of conductance before and after adsorbing the H_2O molecules. Figure 7 exhibits the

DOI: 10.1021/acs.jpcc.5b08771
J. Phys. Chem. C 2015, 119, 28640−28647

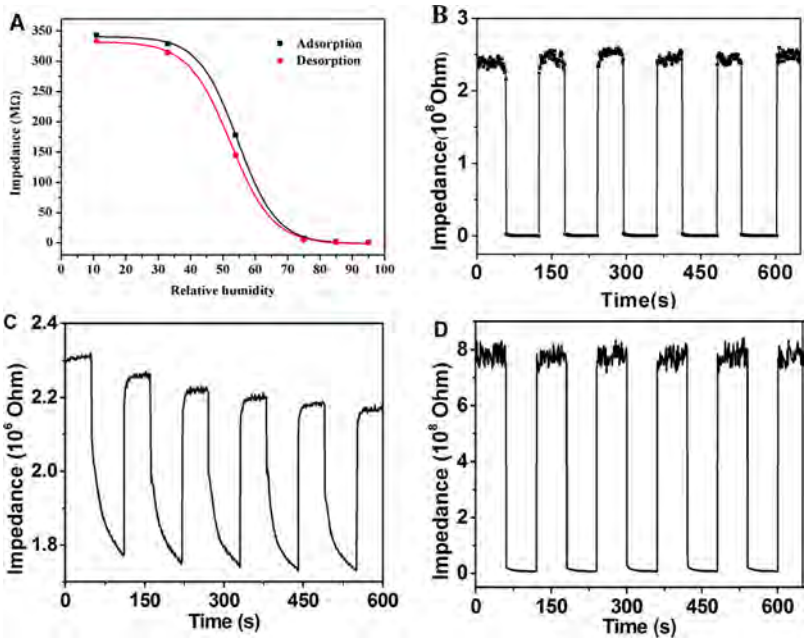

Figure 5. (A) Hysteresis curve of Ag-NA-rGO-based HS. Response and recovery characteristic curves of HS based on (B) Ag-NA-rGO, (C) rGO, and (D) NA-rGO for five cycles under the frequency measured at 100 Hz.

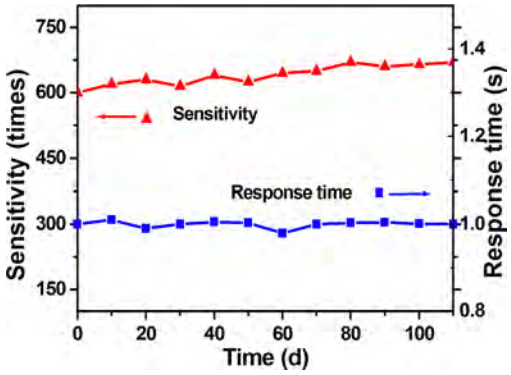

Figure 6. Stability of Ag-NA-rGO composite-based humidity sensor after exposure in air for 110 days.

Table 1. Comparison of Humidity Sensing Characteristics of the Graphene-Based HS

	HS materials based on GO	response and recovery times	stability[a]	ref
1	distinctive 2D structure of GO	~30 ms	72 h	7
2	graphene oxide (GO) films	10.5 and 4.1 s	30 days	42
3	rGO/PDAA composite films	108−147 s and 94−133 s	60 days	17
4	GO/SnOx/CF composites	8 and 6 s	–	8
5	GO/NaPSS bilayer film	3 and 75 s	–	43
6	CuO/rGO composites	2 and 17 s	–	12
7	rGO	50 s	–	this work
8	NA-rGO composites	1 s	–	this work
9	**Ag-NA-rGO composites**	**1 s**	**110 days**	**this work**

[a]A "–" indicates no discussion in the paper regarding stability.

schematic for the H_2O sensing mechanism for Ag-NA-rGO composite. The sensor is a resistive load and the sensing reaction is supposed to take place on only the sensor surface; thus, the impedance can be defined as follows:

$$I = I_s + I_t = I_g + I_t = \frac{I_0}{q\mu_p p} + I_t \quad (1)$$

where I_s and I_t are the impedance brought by the top graphene layer and the signal transfer from the top layer to the electrodes, respectively. I_0 is a constant, q the charge value, μ_p the hole mobility, and p the hole concentration.

When sensors are exposed to H_2O molecules, I_s can be affected, which can be described as follows:

$$I_s = \frac{I_w \times I_g}{I_w + I_g} = \frac{\frac{I_1}{q\mu_{H^+}C_{H^+} + q\mu_{H_3O^+}C_{H_3O^+}} \times \frac{I_0}{q\mu_p p}}{\frac{I_1}{q\mu_{H^+}C_{H^+} + q\mu_{H_3O^+}C_{H_3O^+}} + \frac{I_0}{q\mu_p p}} = \frac{\frac{I_1}{q\mu_{H^+}A_0P_{0H^+} + q\mu_{H_3O^+}A_1P_{1H_3O^+}} \times \frac{I_0}{q\mu_p p}}{\frac{I_1}{q\mu_{H^+}A_0P_{0H^+} + q\mu_{H_3O^+}A_1P_{1H_3O^+}} + \frac{I_0}{q\mu_p p}} \quad (2)$$

where I_1 is a constant; μ_{H^+} and C_{H^+} are the mobility and concentrations of H^+, respectively; and $\mu_{H_3O^+}$ and $C_{H_3O^+}$ are the mobility and concentration of H_3O^+, respectively. A_0 and P_0 are the absorption ratio and productivity for H^+, respectively. A_1 and P_1 are the absorption ratio and productivity for H_3O^+, respectively.

At low RH, H_2O molecules cover the surface discontinuously; thus, electric charges are difficult to transfer. However, the Ag nanoparticles on the rGO surface provide a high local charge density and stronger electrostatic field which promote the dissociation of H_2O molecules and provide H^+ as charge carriers of the hopping transport. Thus, I_s can be further expressed as

DOI: 10.1021/acs.jpcc.5b08771
J. Phys. Chem. C 2015, 119, 28640−28647

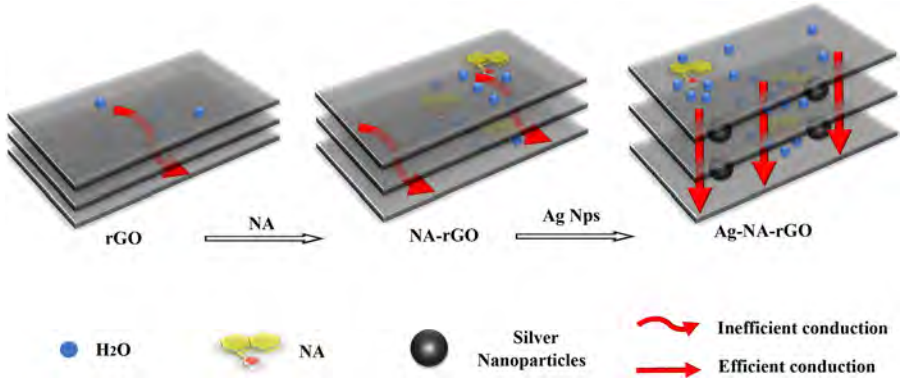

Figure 7. Schematic for the H_2O sensing mechanism for Ag-NA-rGO composite.

$$I_s = \frac{I_w \times I_g}{I_w + I_g} = \frac{\frac{I_1}{q\mu_{H^+}A_0P_{0H^+}} \times \frac{I_0}{q\mu_p p}}{\frac{I_1}{q\mu_{H^+}A_0P_{0H^+}} + \frac{I_0}{q\mu_p p}} \quad (3)$$

When the RH reaches a high value, serial water layers will be formed on the surface of rGO films by a physisorption process. Because hydration of H_3O^+ is energetically favored in liquid water, it can be expected that H_3O^+ will be hydrated if the adsorbed H_2O is sufficient. According to the ion transfer mechanism, $H_2O + H_3O^+ \rightarrow H_3O^+ + H_2O$ is the same on both sides of the equation. Certainly the energy is also equivalent, so the transfer of H_3O^+ is quite easy. At this condition, I_s can be described as

$$I_s = \frac{I_w \times I_g}{I_w + I_g} = \frac{\frac{I_1}{q\mu_{H_3O^+}A_0P_{0H_3O^+}} \times \frac{I_0}{q\mu_p p}}{\frac{I_1}{q\mu_{H_3O^+}A_0P_{0H_3O^+}} + \frac{I_0}{q\mu_p p}} \quad (4)$$

Thus, the sensitivity of the fabricated sensor and the linearity between the sensor impedance and RH values are directly related to the absorption ratios and productivities of the surface films of the sensors. The NA-rGO with high density of active sites and greatly increased interfacial areas between the active sensing regions of the rGO can significantly improve these properties; thus, the fabricated HS exhibited excellent humidity sensing performance.

The ultrafast response of the fabricated Ag-NA-rGO-based HS can be understood schematically by Figure 7. Such an ultrafast response and recovery behavior for the fabricated HS could be ascribed to the large surface area and wide interlayer spacing in the prepared Ag-NA-rGO composite. Theoretically, the ultrafast response of the fabricated HS can be explained by the average speed (ν) of the carriers:[33]

$$\nu = \frac{q\varepsilon}{m}\tau \quad (5)$$

where ε is the electric field intensity and τ is a constant. ε is inversely proportional to the distance between graphene layers. The huge gaps between the graphene layers are fixed by Ag nanoparticles, which can provide convenient channels for the electrical signal transmission through the graphene layers to the electrode substrates. As a result, Ag-NA-rGO is relatively more efficient in conduction than those without Ag nanoparticles. Moreover, the absorption and desorption barrier from the NA surface for H_2O molecules is very low, which also provides faster electron transfer between graphene layers. Because of the absence of Ag nanoparticles, NA-rGO is relatively inefficient in conduction compared to Ag-NA-rGO, but it is much better than rGO.

CONCLUSIONS

Supramolecularly modified graphene (Ag-NA-rGO) composites were prepared, characterized, and used as an efficient material to fabricate highly efficient humidity sensor. The fabricated Ag-NA-rGO composite-based HSs exhibited outstanding humidity sensing characteristics such as ultrafast response and recovery and excellent reproducibility and stability. Such high-performance HSs demonstrate enormous progress in high-speed responsive humidity detection and control. Importantly, the supramolecular assembly technique was utilized, for the first time, to fabricate such in situ reducible, graphene-based multilayer composites with multilevel interfaces for efficient humidity sensing application. Thus, the presented work demonstrates that supramolecularly modified graphene is an excellent material which can be used to fabricate high-performance HSs and other kinds of sensors.

ASSOCIATED CONTENT

Supporting Information

The Supporting Information is available free of charge on the ACS Publications website at DOI: 10.1021/acs.jpcc.5b08771.

Additional data and analyses (PDF)

AUTHOR INFORMATION

Corresponding Author

*E-mail: yao@buaa.edu.cn.

Author Contributions

‖S.W. and Z.C.: These authors contributed equally.

Notes

The authors declare no competing financial interest.

ACKNOWLEDGMENTS

This work was supported by the National Natural Science Foundation of China (Grant 51373005, 21204087), National Key Basic Research Program of China (2014CB931800), Program for New Century Excellent Talents in University (NCET-10-0035), and Fundamental Research Funds for the Central Universities.

REFERENCES

(1) Qiu, Y.; Yang, S. ZnO Nanotetrapods: Controlled Vapor-Phase Synthesis and Application for Humidity Sensing. *Adv. Funct. Mater.* **2007**, *17*, 1345−1352.

DOI: 10.1021/acs.jpcc.5b08771
J. Phys. Chem. C 2015, 119, 28640−28647

(2) Garcia-Belmonte, G.; Kytin, V.; Dittrich, T.; Bisquert, J. Effect of Humidity on the AC Conductivity of Nanoporous TiO_2. *J. Appl. Phys.* **2003**, *94*, 5261−5264.
(3) Shi, J.; Hsiao, V. K.; Huang, T. J. Nanoporous Polymeric Transmission Gratings for High-Speed Humidity Sensing. *Nanotechnology* **2007**, *18*, 465501.
(4) Li, Z.; Zhang, H.; Zheng, W.; Wang, W.; Huang, H.; Wang, C.; MacDiarmid, A. G.; Wei, Y. Highly Sensitive and Stable Humidity Nanosensors Based on LiCl Doped TiO_2 Eelectrospun Nanofibers. *J. Am. Chem. Soc.* **2008**, *130*, 5036−5037.
(5) Kuang, Q.; Lao, C.; Wang, Z. L.; Xie, Z.; Zheng, L. High-Sensitivity Humidity Sensor Based on a Single SnO2 Nanowire. *J. Am. Chem. Soc.* **2007**, *129*, 6070−6071.
(6) Zhan, X.; Yang, M.; Lei, Z.; Li, Y.; Liu, Y.; Yu, G.; Zhu, D. Photoluminescence, Electroluminescence, Nonlinear Optical, and Humidity Sensitive Properties of Poly (p-diethynylbenzene) Prepared with a Nickel Acetylide Catalyst. *Adv. Mater.* **2000**, *12*, 51−53.
(7) Borini, S.; White, R.; Wei, D.; Astley, M.; Haque, S.; Spigone, E.; Harris, N.; Kivioja, J.; Ryhanen, T. Ultrafast Graphene Oxide Humidity Sensors. *ACS Nano* **2013**, *7*, 11166−11173.
(8) Fu, T.; Zhu, J.; Zhuo, M.; Guan, B.; Li, J.; Xu, Z.; Li, Q. Humidity Sensors Based on Graphene/SnO x/CF Nanocomposites. *J. Mater. Chem. C* **2014**, *2*, 4861−4866.
(9) Saab, A. P.; Laub, M.; Srdanov, V. I.; Stucky, G. D. Oxidized Thin Films of C 60: a New Humidity-Sensing Material. *Adv. Mater.* **1998**, *10*, 462−465.
(10) Chen, M.; Zhang, C.; Li, L.; Liu, Y.; Li, X.; Xu, X.; Xia, F.; Wang, W.; Gao, J. Sn Powder as Reducing Agents and SnO_2 Precursors for the Synthesis of SnO_2-Reduced Graphene Oxide Hybrid Nanoparticles. *ACS Appl. Mater. Interfaces* **2013**, *5*, 13333−13339.
(11) Yao, Y.; Chen, X.; Li, X.; Chen, X.; Li, N. Investigation of the Stability of QCM Humidity Sensor Using Graphene Oxide as Sensing Films. *Sens. Actuators, B* **2014**, *191*, 779−783.
(12) Wang, Z.; Xiao, Y.; Cui, X.; Cheng, P.; Wang, B.; Gao, Y.; Li, X.; Yang, T.; Zhang, T.; Lu, G. Humidity-Sensing Properties of Urchinlike CuO Nanostructures Modified by Reduced Graphene Oxide. *ACS Appl. Mater. Interfaces* **2014**, *6*, 3888−3895.
(13) Zhao, S.; Yin, H.; Du, L.; Yin, G.; Tang, Z.; Liu, S. Three Dimensional N-Doped Graphene/PtRu Nanoparticle Hybrids as High Performance Anode for Direct Methanol Fuel Cells. *J. Mater. Chem. A* **2014**, *2*, 3719−3724.
(14) Tang, H.; Yin, H.; Wang, J.; Yang, N.; Wang, D.; Tang, Z. Molecular Architecture of Cobalt Porphyrin Multilayers on Reduced Graphene Oxide Sheets for High-Performance Oxygen Reduction Reaction. *Angew. Chem.* **2013**, *125*, 5695−5699.
(15) Yin, H.; Zhao, S.; Wan, J.; Tang, H.; Chang, L.; He, L.; Zhao, H.; Gao, Y.; Tang, Z. Three-Dimensional Graphene/Metal Oxide Nanoparticle Hybrids for High-Performance Capacitive Deionization of Saline Water. *Adv. Mater.* **2013**, *25*, 6270−6276.
(16) Yin, H.; Tang, H.; Wang, D.; Gao, Y.; Tang, Z. Facile Synthesis of Surfactant-Free Au Cluster/Graphene Hybrids for High-Performance Oxygen Reduction Reaction. *ACS Nano* **2012**, *6*, 8288−8297.
(17) Zhang, D.; Tong, J.; Xia, B. Humidity-Sensing Properties of Chemically Reduced Graphene Oxide/Polymer Nanocomposite Film Sensor Based on Layer-By-Layer Nano Self-Assembly. *Sens. Actuators, B* **2014**, *197*, 66−72.
(18) Li, Y.; Deng, C.; Yang, M. Facilely Prepared Composites of Polyelectrolytes and Graphene as the Sensing Materials for the Detection of very Low Humidity. *Sens. Actuators, B* **2014**, *194*, 51−58.
(19) Hwang, S.-H.; Kang, D.; Ruoff, R. S.; Shin, H. S.; Park, Y.-B. Poly (vinyl alcohol) Reinforced and Toughened with Poly (dopamine)-Treated Graphene Oxide, and its Use for Humidity Sensing. *ACS Nano* **2014**, *8*, 6739−6747.
(20) Karim, M. R.; Hatakeyama, K.; Matsui, T.; Takehira, H.; Taniguchi, T.; Koinuma, M.; Matsumoto, Y.; Akutagawa, T.; Nakamura, T.; Noro, S.-i.; et al. Graphene Oxide Nanosheet with High Proton Conductivity. *J. Am. Chem. Soc.* **2013**, *135*, 8097−8100.
(21) Zhu, J.; Andres, C. M.; Xu, J.; Ramamoorthy, A.; Tsotsis, T.; Kotov, N. A. Pseudonegative Thermal Expansion and the State of Water in Graphene Oxide Layered Assemblies. *ACS Nano* **2012**, *6*, 8357−8365.
(22) Guo, C. X.; Ng, S. R.; Khoo, S. Y.; Zheng, X.; Chen, P.; Li, C. M. RGD-Peptide Functionalized Graphene Biomimetic Live-Cell Sensor for Real-Time Detection of Nitric Oxide Molecules. *ACS Nano* **2012**, *6*, 6944−6951.
(23) Ouyang, F.; Yang, Z.; Xiao, J.; Wu, D.; Xu, H. Electronic Structure and Chemical Modification of Graphene Antidot Lattices. *J. Phys. Chem. C* **2010**, *114*, 15578−15583.
(24) Srinivasan, S.; Je, S. H.; Back, S.; Barin, G.; Buyukcakir, O.; Guliyev, R.; Jung, Y.; Coskun, A. Ordered Supramolecular Gels Based on Graphene Oxide and Tetracationic Cyclophanes. *Adv. Mater.* **2014**, *26*, 2725−2729.
(25) Yu, H.-W.; Kim, H. K.; Kim, T.; Bae, K. M.; Seo, S. M.; Kim, J.-M.; Kang, T. J.; Kim, Y. H. Self-Powered Humidity Sensor Based on Graphene Oxide Composite Film Intercalated by Poly (Sodium 4-Styrenesulfonate). *ACS Appl. Mater. Interfaces* **2014**, *6*, 8320−8326.
(26) Smith, D. K. Dendritic Supermolecules−Towards Controllable Nanomaterials. *Chem. Commun.* **2006**, *1*, 34−44.
(27) Kwan, K.; Cranford, S. W. 'Unsticking'and Exposing the Surface Area of Graphene Bilayers via Randomly Distributed Nanoparticles. *Chem. Phys. Lett.* **2014**, *609*, 65−69.
(28) Tian, J.; Ning, R.; Liu, Q.; Asiri, A. M.; Al-Youbi, A. O.; Sun, X. Three-Dimensional Porous Supramolecular Architecture from Ultrathin g-C3N4 Nanosheets and Reduced Graphene Oxide: Solution Self-Assembly Construction and Application as a Highly Efficient Metal-Free Electrocatalyst for Oxygen Reduction Reaction. *ACS Appl. Mater. Interfaces* **2014**, *6*, 1011−1017.
(29) Park, Y. D.; Kang, B.; Lim, H. S.; Cho, K.; Kang, M. S.; Cho, J. H. Polyelectrolyte Interlayer for Ultra-Sensitive Organic Transistor Humidity Sensors. *ACS Appl. Mater. Interfaces* **2013**, *5*, 8591−8596.
(30) Vijayan, A.; Fuke, M.; Hawaldar, R.; Kulkarni, M.; Amalnerkar, D.; Aiyer, R. Optical Fibre Based Humidity Sensor using Co-Polyaniline Clad. *Sens. Actuators, B* **2008**, *129*, 106−112.
(31) Rezania, B.; Severin, N.; Talyzin, A. V.; Rabe, J. r. P. Hydration of Bilayered Graphene Oxide. *Nano Lett.* **2014**, *14*, 3993−3998.
(32) Huh, S. H. X-ray Diffraction of Multi-Layer Graphenes: Instant Measurement and Determination of the Number of Layers. *Carbon* **2014**, *78*, 617−621.
(33) Andrei, E. Y.; Li, G.; Du, X. Electronic Properties of Graphene: A Perspective from Scanning Tunneling Microscopy and Magneto-Transport. 2012, arXiv:1204.4532. arXiv.org e-Print archive.
(34) Guo, X.; Du, K.; Ge, H.; Guo, Q.; Wang, Y.; Wang, F. Good Sensitivity and High Stability of Humidity Ssensor using Micro-arc Oxidation Alumina Film. *Electrochem. Commun.* **2013**, *28*, 95−99.
(35) Jiang, K.; Fei, T.; Zhang, T. Humidity Sensing Properties of LiCl-Loaded Porous Polymers with Good Stability and Rapid Response and Recovery. *Sens. Actuators, B* **2014**, *199*, 1−6.
(36) Miyoshi, Y.; Miyajima, K.; Saito, H.; Kudo, H.; Takeuchi, T.; Karube, I.; Mitsubayashi, K. Flexible Humidity Sensor in a Sandwich Configuration with a Hydrophilic Porous Membrane. *Sens. Actuators, B* **2009**, *142*, 28−32.
(37) Liang, Q.; Xu, H.; Zhao, J.; Gao, S. Micro Humidity Sensors Based on ZnO−In_2O_3 Thin Films with High Performances. *Sens. Actuators, B* **2012**, *165*, 76−81.
(38) Qi, Q.; Zhang, T.; Wang, L. Improved and Excellent Humidity Sensitivities Based on KCl-Doped TiO2 Electrospun Nanofibers. *Appl. Phys. Lett.* **2008**, *93*, 023105.
(39) Huang, L.; Wang, Z.; Zhang, J.; Pu, J.; Lin, Y.; Xu, S.; Shen, L.; Chen, Q.; Shi, W. Fully Printed, Rapid-Response Sensors Based on Chemically Modified Graphene for Detecting NO2 at Room Temperature. *ACS Appl. Mater. Interfaces* **2014**, *6*, 7426−7433.
(40) Li, Y. Q.; Yu, T.; Yang, T. Y.; Zheng, L. X.; Liao, K. Bio-Inspired Nacre-Like Composite Films Based on Graphene With Superior Mechanical, Electrical, and Biocompatible Properties. *Adv. Mater.* **2012**, *24*, 3426−3431.
(41) Chen, Z.; Umar, A.; Wang, S.; Wang, Y.; Tian, T.; Shang, Y.; Fan, Y.; Qi, Q.; Xu, D.; Jiang, L. Supramolecular Fabrication of

DOI: 10.1021/acs.jpcc.5b08771
J. Phys. Chem. C 2015, 119, 28640−28647

Multilevel Graphene-Based Gas Sensors with High NO_2 Sensibility. *Nanoscale* **2015**, *7*, 10259−10266.
(42) Bi, H.; Yin, K.; Xie, X.; Ji, J.; Wan, S.; Sun, L.; Terrones, M.; Dresselhaus, M. S. Ultrahigh Humidity Sensitivity of Graphene Oxide. *Sci. Rep.* **2013**, *3*, 2714.
(43) Huang, H.; Sun, A.; Chu, C.; Li, Y.; Xu, G. Electrical and Humidity Sensing Properties of Graphene and Polystyrene Sulfonic Sodium Bilayer Thin Film. *Integr. Ferroelectr.* **2013**, *144*, 127−134.

DOI: 10.1021/acs.jpcc.5b08771
J. Phys. Chem. C 2015, 119, 28640−28647